

# A Contribution to CESE method validation in LS-DYNA<sup>®</sup>

Edith GRIPPON<sup>1</sup>, Nicolas VAN DORSSELAER<sup>1</sup>, Vincent LAPOUJADE<sup>1</sup>

<sup>1</sup>DynaS+, 5 Avenue Didier Daurat, 31400 TOULOUSE, France

## 1 Introduction

In fluid mechanics, a compressible flow is said when the density varies during a pressure change. Empirically, it is considered that when Mach > 0.3 the flow is compressible. In this case, shock waves, contact discontinuities and relaxation can appear when an obstacle is encountered.

Since LS-DYNA R7, a new CESE method is available. Several finite element studies were performed by DynaS+ to evaluate the precision of this method in pure CFD studies and to confirm good abilities in Fluid Structure Interaction studies (Figure 1).

Pure fluid cases were tested on strong shocks and expansion studies. Results were compared to experimental data extracted from reference papers. The very good precision obtained with the CESE solver and its ability to represent very dynamic phenomenon will be shown.

Fluid Structure Interaction in 2D was tested with a deformable plate. Results (also compared with experimental data extracted from a reference paper) will be presented and will highlight that the Coupling method in 2D is as efficient as in 3D.

	CESE :	ICFD :	ALE :
Low speed aerodynamics (turbulence)	-	✓	-
High speed aerodynamics (shock waves)	✓	-	-
Explosions using JWL EOS or similar	-	-	✓
Airbags-Pistons	✓	-	✓
Free surface problems (slamming)	-	✓	✓
FSI capabilities	✓	✓	✓
Chemistry reactions	✓	-	-
Stochastic particles	✓	-	-

Figure 1: case of application of different methods of modeling fluids in LS-DYNA [1]

In order to better understand the different validation cases presented later in this paper (1D, 2D, 2D fluid structure interaction), a very brief reminder on the phenomena that govern compressible flow and rapid introduction of the resolution method implemented the CESE solver are presented in this introduction.

### 1.1.1 Shock, contact discontinuity and expansion

When supersonic flow encounters an obstacle, three phenomena related to fluid compressibility can be identified (Figure 2):

- The upstream fluid particles do not have the information that there is a concave downstream obstacle. The streamlines do not have the time to adapt; a shock wave is created with increasing Mach number and pressure.

- If the obstacle is convex, the current lines do not adapt to the shape of the obstacle. This produces an isentropic phenomenon called expansion which is the opposite of the chock and causes a reduction of the Mach number and pressure.
- The third phenomenon related to transonic and supersonic flows is contact discontinuity that can be imagined as a fictional membrane separating two fluids. There is no flow of material through this discontinuity, the speed and pressure are thus continuous through the contact discontinuity but the density and temperature are discontinuous.

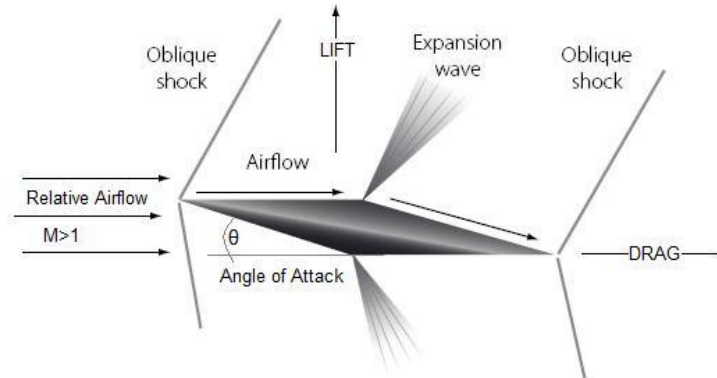


Figure 2: Expansion Waves & Oblique shock for concave and convex obstacle

### 1.1.2 CESE method in LS-DYNA

The CESE solver is a compressible flow solver based upon the Conservation Element/Solution Element (CE/SE) method, originally proposed by Dr. Chang in NASA Glenn Research Center [2]. This method is an innovative numerical framework for the resolution of conservation laws. It has many non-traditional features, including a unified treatment of space and time, the introduction of conservation element (CE) and solution element (SE), and a novel shock capturing strategy without using a Riemann solver (Figure 3).

The CE/SE method implemented in LS-DYNA is explicit and more accurate than classical 2nd order scheme and has several unique features like [3]:

- Flux conservations in space-time (locally & globally),
- Spatial derivatives are treated as unknown, which allows to have very specific solutions and more precision,
- Simple but very effective shock-capturing strategy, no Riemann solver is needed (very expensive in computing time),
- Flexible element shape,
- Both strong shocks and small disturbances can be handled very well simultaneously.
- The simplicity of the CE/SE schemes makes the computer programs easy to vectorize and parallelize.

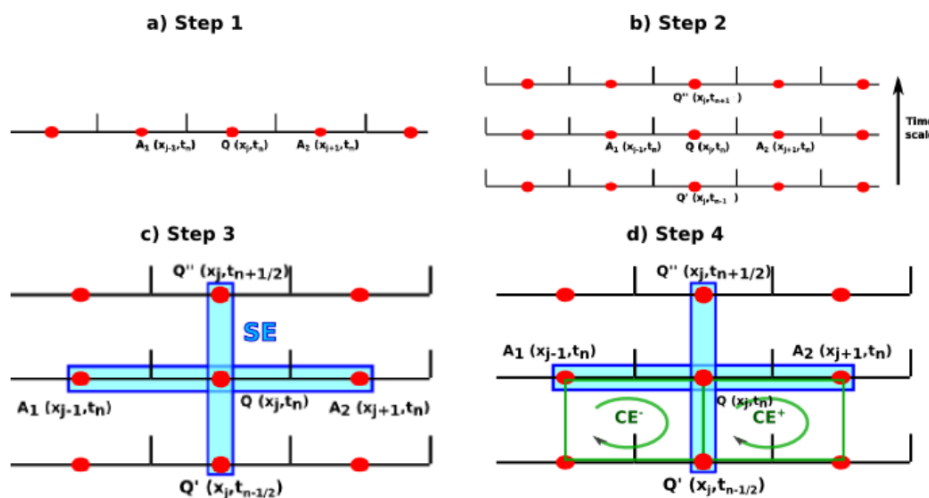


Figure 3: CESE method: example of CESE 1D resolution scheme [4]. Step 1: element discretization, step 2: expansion in the time dimension, step 3: definition of a SE and step 4 definition of the CE

For nonlinear equations, some numerical diffusion should be added, then we can get a modified scheme ( $\epsilon$  scheme). For flows with discontinuities, especially with shocks, a re-weighting procedure (limiter) should be applied ( $\alpha$ - $\beta$  scheme), which is the approach used by the CESE solver. In fluid/structure coupling, a quasi-constraint method is used. For the fluid part, the CE/SE method just described is used based upon an Eulerian frame, while for the structural parts, the FEM solver in LS-DYNA is employed based upon the Lagrangian frame. Both fluid and structure meshes are independent (more accurate if the fluid mesh size is smaller than the structural mesh size). The interface boundary locations and velocities are dictated by the Lagrangian structure. This information will be used by the fluid solver as the interface conditions at each time step, and the CE/SE solver feeds back the fluid pressures (forces) on the structural interface as exterior forces for the structural solver [5].

## 2 Validation cases

Several validation cases for the CESE numerical scheme can be found on the LSTC website [6]. So far, this method has been used to solve many different types of flow problems, such as detonation waves, shock/acoustic wave interaction, cavitating flows, and chemical reaction flows.

The solver CESE has proven itself on cases of shock, expansion, interaction shock/shock, expansion/shock and expansion/expansion. The purpose of the tests presented in this paper is to compare the CESE solver in terms of performance with dedicated specialist solvers of the domain.

### 2.1 1D Problem

The two cases presented in this paper are classic 1-D models, corresponding to variant of shock tube [7]. For both, the main purpose is to verify the ability of the CESE solver to effectively solve fluid dynamics problems with strong or/and interaction between discontinuities due to the compressive behavior of the flow [8]. These 1D models correspond to simple data set for which the computation time (less than 1 minute) allow for extensive testing. Most of the time the 1D case has an analytical solution, which allows comparison with real and physical data depending on any parameter.

#### 2.1.1 Pressure Jump 5 orders of magnitude

The first test case consists of a tube closed at both ends, with a diaphragm separating a region of high-pressure gas on the left from a region of low pressure gas on the right (Figure 4). When the diaphragm is removed, an expansion wave travels to the left and a shock wave to the right (Figure 5). Analytical solutions exist that permit the description of the behavior of the velocity, pressure or density variables along the horizontal axis at a given time [9]. The pressure jump of 5 orders of magnitude causes displacement of shock wave in direction of the increasing  $x$ . This high pressure jump creates very strong discontinuity challenging the CESE solvers. In addition, the contact discontinuity and the shock are very close, making the capture of the phenomenon even more difficult [10].

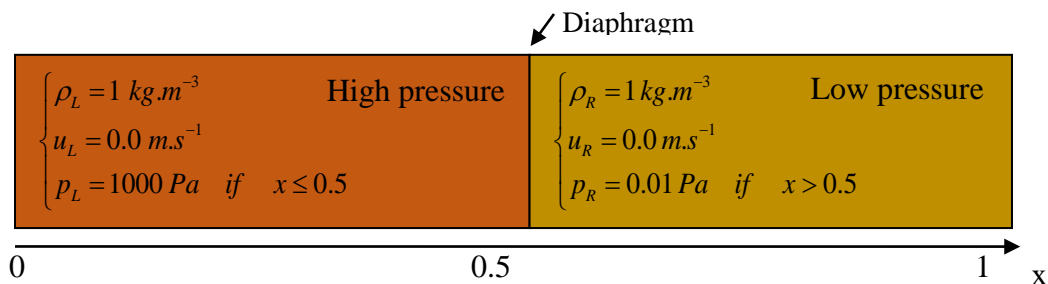


Figure 4: Initial state in the shock tube

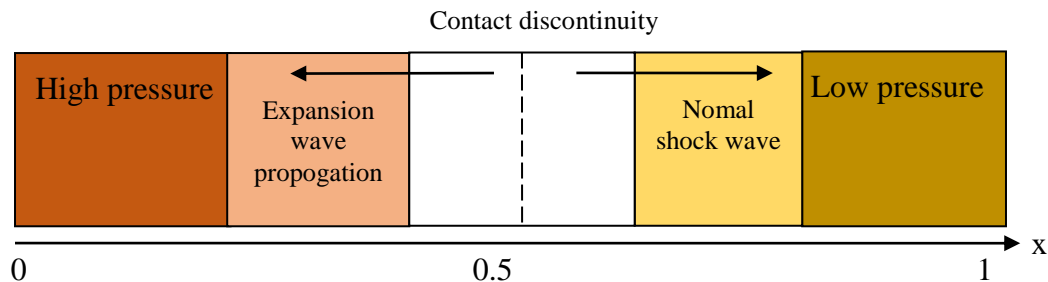


Figure 5: Flow in a shock tube after the diaphragm is broken

Figure 6 represents the evolution of the density at  $t=0,012s$  as a function of number of elements in the mesh. Several meshes were tested from 100, 200, 500 to 1000 uniform elements, which corresponds respectively to mesh sizes of 10 mm; 5 mm; 2 mm; 1 mm. There is a convergence of the LS-DYNA solution when the number of elements increases. For 500 elements, the level of plateau is captured by the solver and solution shows good agreement between numerical results and analytical solution for a double close discontinuity.

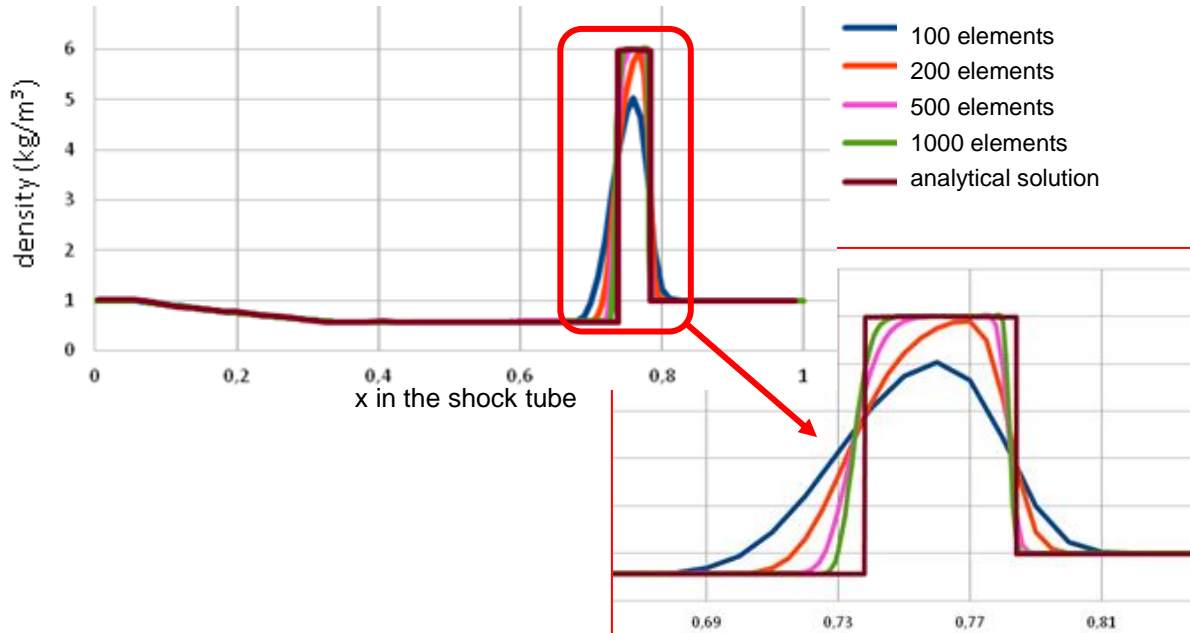


Figure 6: Evolution of the density at  $t=0,012s$  as a function of number of elements in the mesh

Figure 7 shows the evolution of the pressure as a function of distance in the tube, the pressure is continuous through the contact discontinuity. The results are relatively accurate even for a 100 element mesh. The CESE solver captures satisfactorily discontinuities when they are not close together. However, oscillations are still visible near discontinuities (especially around  $x = 0.4m$ ). These oscillations are typical of the 2 order resolution scheme used, which no resolution method type Total Variation Diminishing (TVD). The zoom Figure 7 shows that when the mesh is refined, this oscillation is reduced.

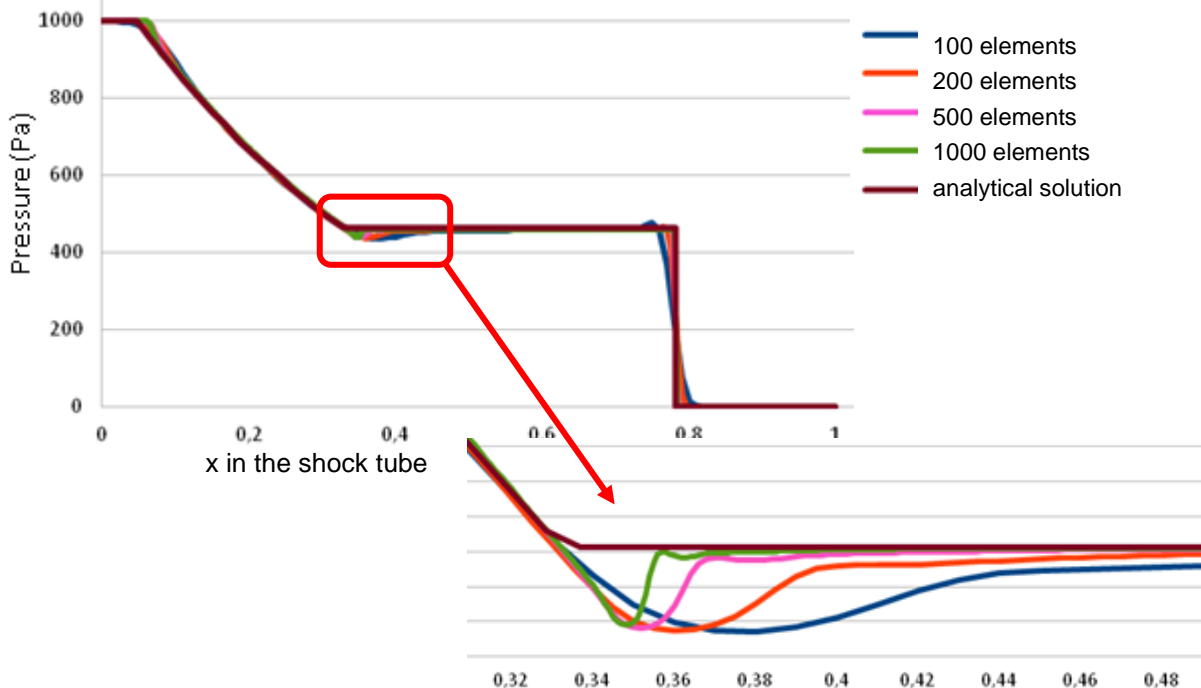


Figure 7: Evolution of the pressure profile at  $t=0.012s$

2.1.2 Interaction between two shock waves

This second shock tube problem was originally proposed by Woodward and Colella [11]. The closed tube has two diaphragm at  $x = 0.1\text{m}$  and  $x = 0.9\text{m}$  are simultaneously opened at  $t=0\text{s}$  (Figure 8). For our study, it was used to compare the CESE solver performance with other solvers specialized in fluid mechanics phenomena involving shocks. This problem has no analytic solution, but a digital reference solution was implemented with an exact Riemann solver and a large number of elements.

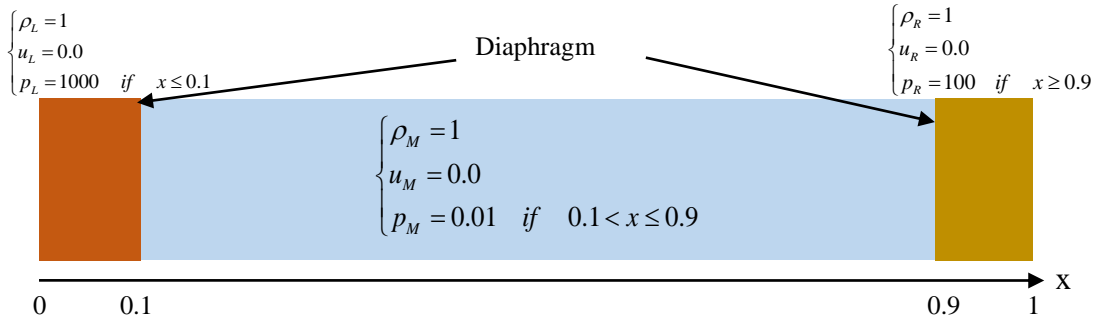


Figure 8: Initial state in the shock tube with 2 diaphragms

Pressure discontinuities on each side will lead to the formation of shock waves of different intensities, propagating toward the central zone of the tube. On both sides, the expansions will be reflected on the ends of the tube and come to interact with the shock waves. From time  $t = 0.028\text{s}$ , the shock waves collide, reflected expansion catches shock waves, making pressure, density, speed profile particularly complex.

Behind each shock wave, there is a contact discontinuity. Collisions between shocks, expansions and contact discontinuities create particularly strong density peaks. Figure 9 shows the profile of densities for  $t = 0.038\text{s}$  after numerous interactions between discontinuities.

Figure 9 (a), to compare the CESE solver with both the reference exact Riemann solution and results from solver HLLC (Harten-Lax-Van Leer-Contact), a 400 element mesh was selected. Both CESE solver stabilization methods were used. The epsilon method has very similar results to the HLLC solver. For these different solvers, with 400 elements in the mesh, the amplitude of the peak around 0.8m is not correctly reproduced. A mesh convergence study was therefore made (Figure 9 (b)). A very good convergence with the exact Riemann solver is observed from 800 elements.

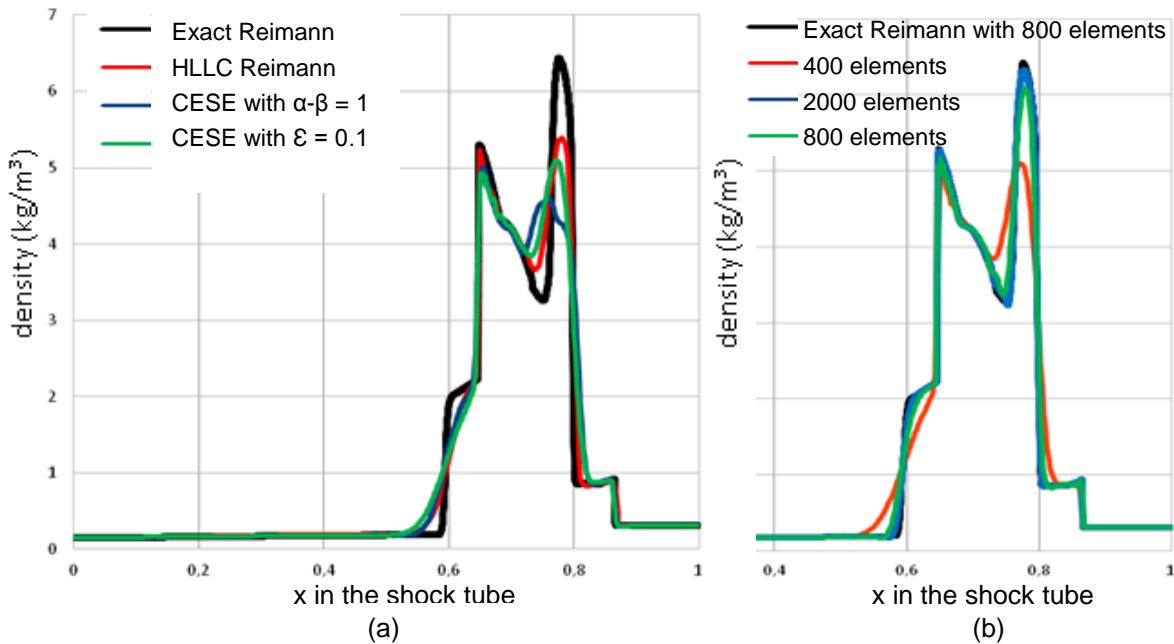


Figure 9: (a) comparison of the CESE solver (with  $\alpha\text{-}\beta$  and  $\epsilon$  stabilization method) and the solver HLLC with a 400 element mesh with the exact Riemann solver, (b) comparison to the CESE solver for mesh convergence study

## 2.2 2D Problem

The default for CESE solver in LS-DYNA is 3D. But an option for 2D problem calculations is given using a mesh that has only a single layer of elements and no boundary conditions in the z-direction. 2D problem calculations save a lot of CPU time for some cases.

### 2.2.1 Oblique shock

A simple case of a two-dimensional supersonic flow meeting a cone was chosen for various reasons:

- the presence of well-defined analytical solution in literature (Rankine-Hugoniot equation [12]),
- the presence of result from other solver of fluid mechanics: WIND (the NASA solver).

This 2D test problem begins with an incoming supersonic flow at Mach 2.5. This supersonic flow reaches a cone of 15 degrees (Figure 10). The fluid flow is considered as perfect to overcome the viscosity conditions on the wall. To avoid introducing of additional error, the mesh is very fine. The model is 1.5 m long with a mesh size of 3.1mm.

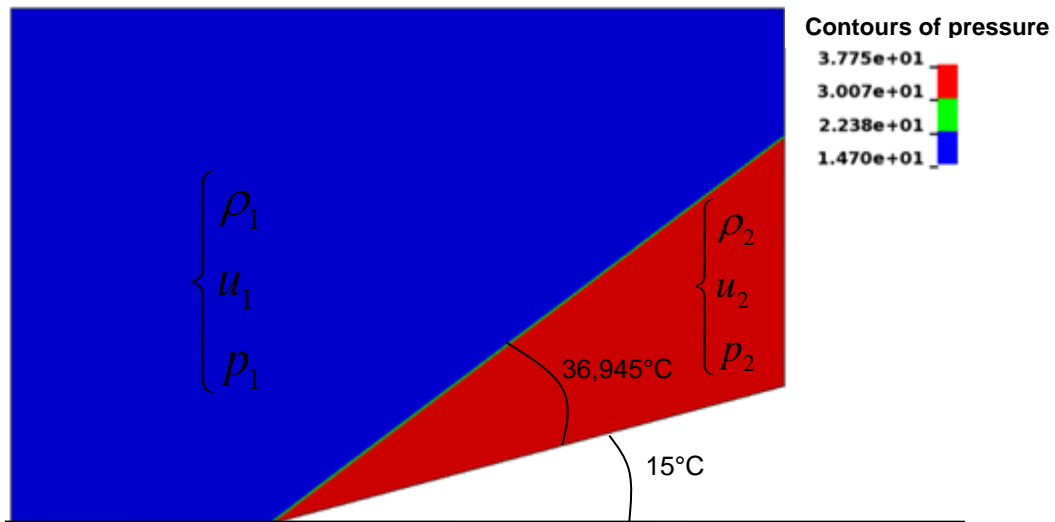


Figure 10: model geometry and contours of pressure, diffraction of a shock wave around a 15° corner

As mentioned above, the CESE solver used by LS-DYNA is associated with two stabilization methods:

- the first uses the parameter  $\epsilon$ , increase this parameter allows to stabilize the calculation at the expense of accuracy. For this study,  $\epsilon = 0.025$ .
- the second a re-weighting procedure (limiter) ( $\alpha$ - $\beta$  scheme) with recommended value of  $\beta = 1$  and  $\alpha = 2$  in the presence of shock waves.

The solver WIND-US is associated by default to a scheme of Roe.

The solver Wind-US and the CESE solver are compared among themselves and with the analytical solution. The errors  $e$  are calculated relative to the analytical solution as follows:

$$e = \left| \frac{\lambda - \lambda_{analytic}}{\lambda_{analytic}} \right| \quad (1)$$

Were  $\lambda$  represent the flow parameter in this case the pressure  $p$ , the temperature  $T$  or the density  $\rho$ . Table 1 summarizes the results obtained for this study. Compared with the analytical results, errors of the CESE solver do not exceed 0.03%.

	analytic	LS-DYNA with $\epsilon$ method	ERREUR (%)
<b>angle</b>	36.945	36.937	<b>0,022</b>
<b>Pressure ratio (p2/p1)</b>	2,4675	2,4676	<b>0,006</b>
<b>Density ratio (rho2/rho1)</b>	1,866549	1,866842	<b>0,016</b>
<b>Temperature ratio (T2/T1)</b>	1,321958	1,321878	<b>0,006</b>

Table 1: Comparison between analytical and numerical results

	analytic	LS-DYNA $\epsilon$	error (%)	LS-DYNA $\alpha - \beta$	error (%)	WIND	error (%)
<b>Post-shock average Mach</b>	1,873526	1,8729	<b>0,0322</b>	1.8719	0.0883	1.8742	<b>0.0371</b>

Table 2: Comparison between analytical and numerical results from LS-DYNA and WIND solver

In Table 2, the average post-shock Mach was compared between the both solvers to observe the precision close and far from the shock. On average, the WIND-US solver has a more accurate post-shock Mach than the CESE solver. The WIND solver is more accurate far of the shock, while the CESE solver is more accurate near the post-shock (Figure 11).

Figure 11 shows a comparison between the analytical response and solvers CESE and WIND for an equivalent mesh. LS-DYNA better capture the shock wave and the value of Mach number is very close to the analytical solution whatever the stabilization method. The epsilon method is generally more accurate than the method  $\alpha - \beta$ . However, the method  $\epsilon$  is oscillating, this is explained by the fact that the choice of the very small epsilon, near the limit of stability.

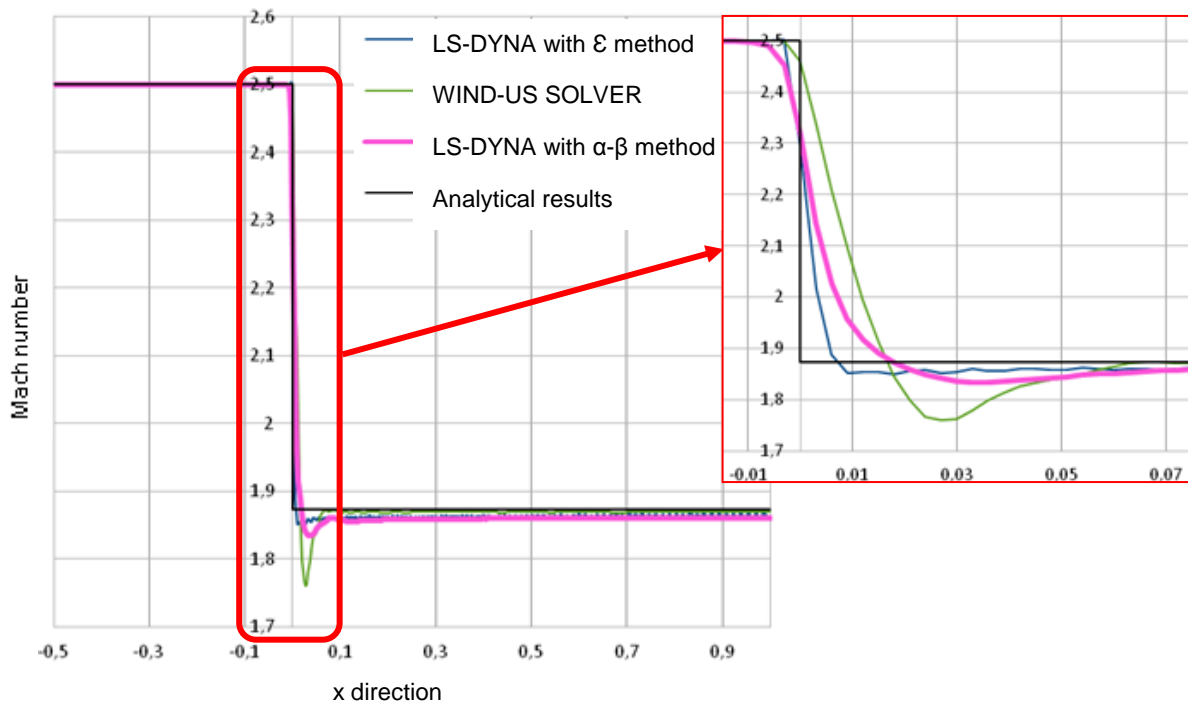


Figure 11: comparison of the Mach number values for the analytical response, CESE and WIND solver for an equivalent mesh

### 3 An introduction to Fluid-Structure Interaction Oblique shock

Because of the lack of fluid-structure interaction FSI validated cases of the CESE solver, different tests were made. The reference study of the behavior of a cantilever panel submitted to a shock tube flow is presented with comparison of numerical and experimental data [13], [14]. The purpose is to confront the CESE solver to an unsteady FSI problem.

#### 3.1 Shock wave impacts on deforming panel

This case study is the propagation of a shock wave on top of a cantilever panel in a non-deformable shock tube, figure 12. The panel length is 50mm and its thickness is 1mm. A transonic flow will spread in the shock tube. The input data; Density, pressure and speed; are shown in (2):

$$\rho = 1,6458 \frac{kg}{m^3} \quad u = 112,61 \frac{m}{s} \quad p = 10000 Pa \quad (2)$$

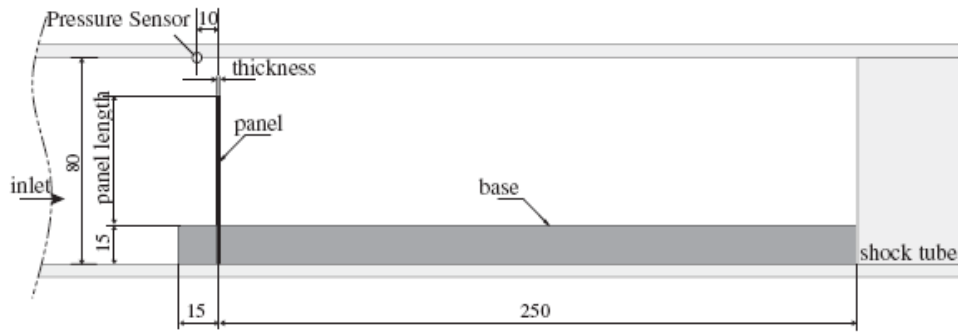


Figure 12: FSI set-up (all dimensions are in millimeters)

When the incident shock wave interacts with the structure, reflected and transmitted shock waves appear at  $t = 0$  s. Behind the panel, the fluid flow encounters a sudden area increase and it undergoes a transition to a cylindrical shock front at  $t = 70 \mu\text{s}$  and after  $t = 280 \mu\text{s}$  it undergoes a transition Regular Reflection toward Mach Reflection. In front of the panel, two reflected shock waves can be distinguished: the first one is due to the interaction with support corner and the second one with the moving panel. One can note that a vortex is produced by the roll-up of the slipstream initiated from the panel ending. The average velocity of this main vortex is about  $115 \text{ m}\cdot\text{s}^{-1}$  and the Strouhal number may be estimated at 1.15. A shock wave attached to the vortex appears. Then, the vortex grows and splits the reflected shock waves as soon as it encounters these ones. At ( $t = 700 \mu\text{s}$ ) a second vortex appears and coalesces with the principal one at ( $t = 910 \mu\text{s}$ ). A third vortex appears at ( $t = 910 \mu\text{s}$ ). On the experimental pictures at  $t = 70 \mu\text{s}$  and  $280 \mu\text{s}$ , three dimensional perturbations due to leaks between the panel and the shock tube walls are also observed.

Figure 13 (a) shows the experimental results at different times, Figure 13 (b) shows the associated digital images (number of Schlieren). The number of Schlieren is a visual comparison of the evolution of shock waves. The complex phenomenon is very well reproduced by LS-DYNA (Digital times and publication do not overlap perfectly).

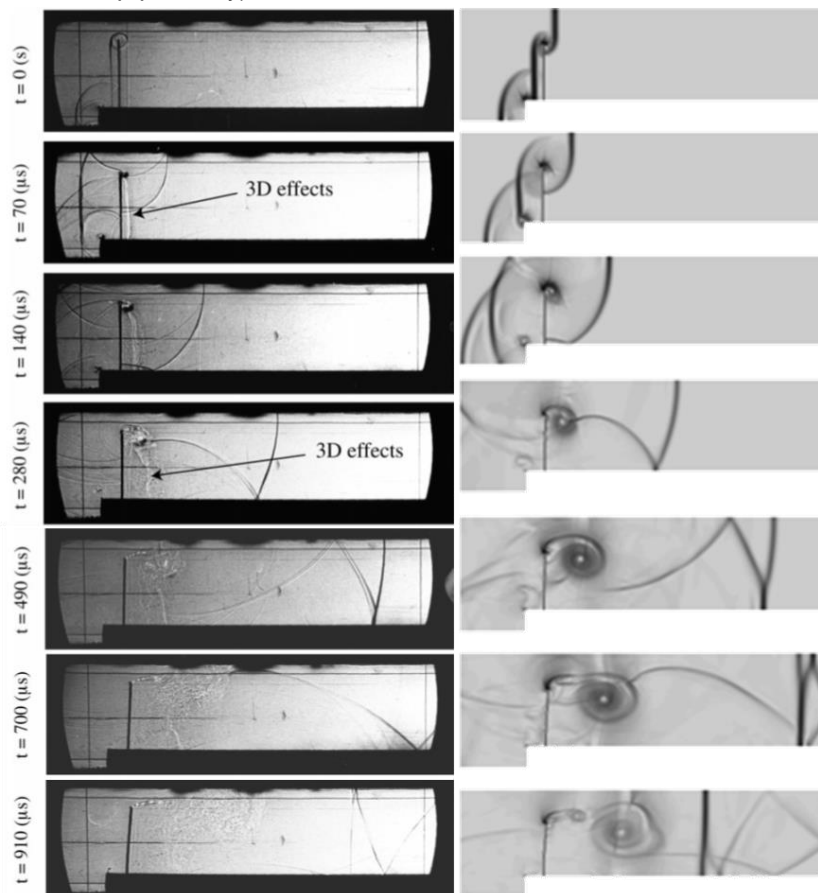


Figure 13: Comparison of (left) experimental Shadowgraph (high speed camera) and (right) numerical Schlieren

Once the first shock wave created, the panel will deform and the shock waves will reflect off the walls by creating multiple interactions. The period and amplitude of the oscillation of the deformable panel are then measured. In Figure 14, the experimental curve of the panel motion is compared to the data obtained by LS-DYNA. The numerical results are very close to experimental data: the experimental period of the panel is 1.9 ms, the calculated period is 1.95 ms.

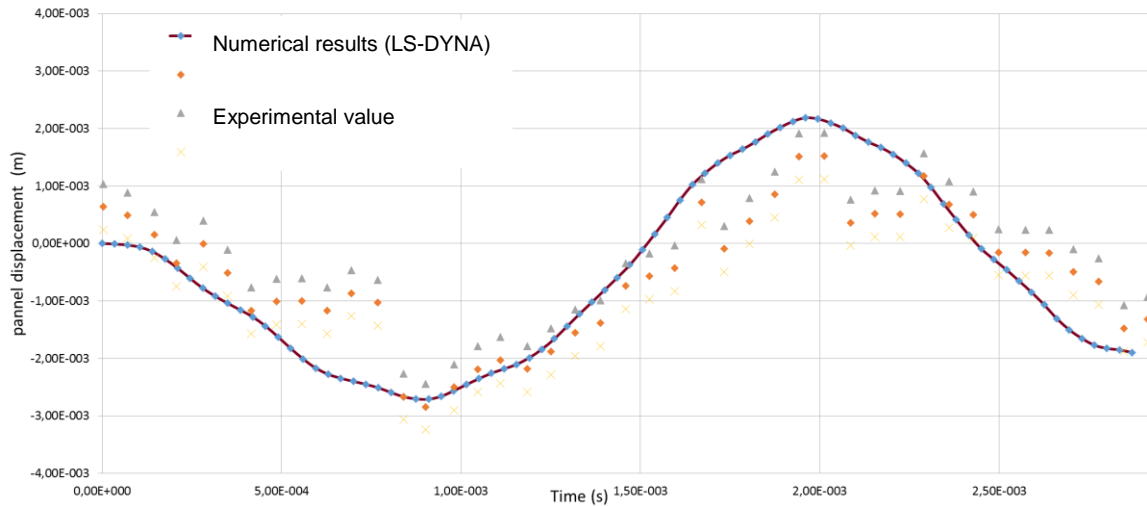


Figure 14: Numerical and experimental 50 mm panel motion

Figure 15 shows a comparison between the experimentally measured pressure at the pressure sensor and the calculated pressure. The first pressure peak is related to the shock wave reflected on the panel and then the second big shock occurs in the transmitted wave. The panel oscillates creating numerous shock waves that oscillate pressure. The experimental data are very noisy; however, LS-DYNA follows correctly the experimental behavior.

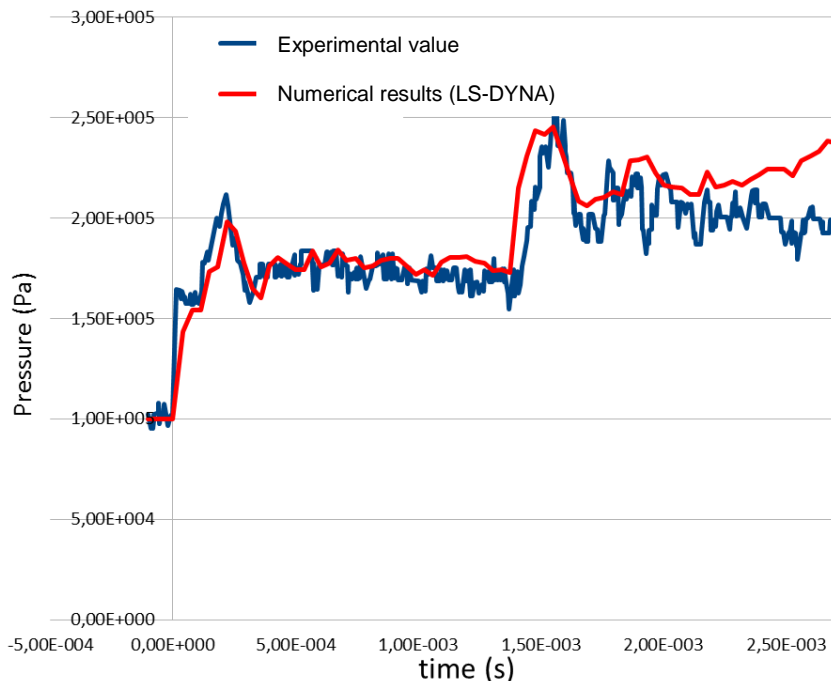


Figure 15: Time evolution of pressure at sensor 1 for the panel

This complex case of fluid-structure interaction is challenging both the mechanic solver, fluid solver and the coupling algorithms. The numerical results for the panel are in relatively good agreement with experiments, as the different criteria show. Shocks and vortices are correctly captured and although our code does not contain any turbulent model, the whole fluid flow is correctly described.

## 4 Conclusion

The comparison between the different models (analytical, numerical) and experiments has shown the good accuracy of CESE solver.

The 1D cases have validated the capture of the different discontinuities related to a compressible flow: shock, expansion, and contact discontinuities. When discontinuities are not very close, the results are very reliable. Moreover, interaction between shock waves and a complex phenomenon demonstrates the robustness of the CESE solver. The 2D cases involving shock waves and expansions have revealed high accuracy of the calculation code.

Finally, the coupling between the mechanical solver and the CESE solver allows fluid-structure interaction studies. The results obtained by the LS-DYNA code correlate well with the experimental data in reasonable computation time (strong coupling highly parallelized).

To continue validation case study of the CESE solver, more device and numerical studies should be proposed to answer to an increase needs of industrial and in the same way a three dimensional study should be made.

## 5 Acknowledgment

M. Iñaki ÇALDICHOURY and Dr. Zeng-Chan ZHANG of LSTC are acknowledged for their helpful comments and suggestions.

## 6 Literature

- [1] Zeng Chan Zhang, Kyoung Su Im, Iñaki Çaldichoury, Compressible CFD (CESE) module presentation, 9th European LS-DYNA Conference, Manchester, 2013
- [2] CHANG Z.C., "The Method of Space-Time Conservation Element and Solution Element – A New Approach for Solving the Navier Stokes and Euler Equations." J. Comput. Phys., Vol. 119, p.295, 1995
- [3] <http://www.grc.nasa.gov/WWW/microbus/>
- [4] Zeng-Chan Zhang, Iñaki Çadichoury, LS-DYNA R7: Recent developments, application areas and validation results of the compressible fluid solver (CESE) specialized in high speed flows, 9th European LS-DYNA Conference, Manchester, 2013
- [5] ZHANG Z.C., CHANG S.C. and YU S.T. (2001). "A Space-Time Conservation Element and Solution Element for Solving the Two- and Three-Dimensional Unsteady Euler Equations Using Quadrilateral and Hexagonal Meshes," J. Comput. Phys., Vol. 175, pp.168-199.
- [6] [http://www.lstc.com/applications/cese\\_cfd/test\\_cases/supersonic](http://www.lstc.com/applications/cese_cfd/test_cases/supersonic)
- [7] G. Sod, A survey of several finite difference methods for systems of nonlinear hyperbolic conservation laws, J. Comput. Phys., 1978
- [8] Inaki Caldichoury, Zeng Chan Zhang, 1-D Shock Tube Problem, STC-QA-LS-DYNA-CESE-VER-1.1-, 2012
- [9] J. D. Anderson, Modern Compressible Flow with historical perspective, Mc Graw Hill, 2003.
- [10] E.F.Toro, Riemann Solvers and Numerical Methods for Fluid Dynamics. A Practical Introduction, 1999
- [11] P. Woodward, P. Colella, The Numerical Simulation of Two-Dimension Fluid Flow with Strong Shocks, Journal of Computational Physics 54, 115.173 (1984)
- [12] J. D. Anderson, modern compressible flow, McGraw Hill Inc., New York, 1982
- [13] Jourdan G., Houas L., Schwaederlé L., Layes G., Carey R., Diaz F.: A new variable inclination shock tube for multiple investigations, Shock Waves, 2003
- [14] J. Giordano, G. Jourdan, Y. Burtshell, M. Medale, D.E. Zeitoun, L. Houas, Shock wave impacts on deforming panel, an application of fluid-structure interaction, Digital Object Identifier (DOI) 10.1007/s00193-005-0246-9, shock wave, 2005